

## Subcellular distribution of the TSC2 gene product tuberin in human airway smooth muscle cells is driven by multiple localization sequences and is cell-cycle dependent

Debbie Clements,<sup>1</sup> R. John Mayer,<sup>2</sup> and Simon R. Johnson<sup>1</sup>

<sup>1</sup>Division of Therapeutics and Molecular Medicine, University of Nottingham, Queens Medical Centre, University Hospital, and <sup>2</sup>Division of Biomedical Sciences, University of Nottingham, Nottingham, United Kingdom

Submitted 15 August 2005; accepted in final form 31 July 2006

**Clements D, Mayer RJ, Johnson SR.** Subcellular distribution of the TSC2 gene product tuberin in human airway smooth muscle cells is driven by multiple localization sequences and is cell-cycle dependent. *Am J Physiol Lung Cell Mol Physiol* 292: L258–L266, 2007. First published August 11, 2006; doi:10.1152/ajplung.00354.2005.—The products of the tuberous sclerosis complex (TSC) genes, hamartin and tuberin (TSC1 and 2), form a heteromer, which represses the kinase mammalian target of rapamycin. Loss of TSC1 or 2 results in diseases characterized by loss of cell-cycle control, including TSC and lymphangioleiomyomatosis. As tuberin has multiple signaling inputs, including phosphatidylinositol-3-OH kinase, mitogen-activated protein kinase, and adenosine monophosphate kinase, we postulated tuberin would have multiple protein interactions governed by subcellular localization and cellular status and examined this in primary human airway smooth muscle cells. Using immunofluorescence and confocal microscopy, tuberin was detected in cytoplasm, nucleus, nucleoli, and mitochondria. Fractionation of synchronized airway smooth cells showed that tuberin enters the nucleus in late G<sub>1</sub>, and passage through the cell cycle is necessary for nuclear entry. Deletion constructs showed localization sequences for the nucleus between amino acids 1351 and 1807, for mitochondria between 901 and 1350, and for cytoplasmic speckles between 1 and 450. Using fluorophore-tagged proteins, we observed fluorescence resonance energy transfer between tuberin and hamartin within these speckles, indicating a direct interaction between the proteins at this site. The observations that tuberin is localized to mitochondria and translocated to the nucleus in G<sub>1</sub> are novel and consistent with interactions with proteins within multiple signaling pathways. Dynamic relocalization of tuberin may control these interactions to integrate these pathways. As tuberin has potential roles in proliferation, migration, and cell phenotype, it therefore warrants further investigation in diseases categorized by abnormalities in airway smooth muscle.

tuberous sclerosis; mitochondria; fluorescence resonance energy transfer

HAMARTIN AND TUBERIN, THE products of tuberous sclerosis complex (TSC) 1 and TSC2 genes, respectively, form a complex, which has recently been recognized as an important repressor of the kinase mammalian target of rapamycin (mTOR) and hence growth factor signaling via phosphoinositide 3-OH kinase (PI3K) and Akt. In response to growth factors, phosphorylation of tuberin at multiple sites by Akt results in disruption of the tuberin/hamartin complex, allowing activation of mTOR, and its downstream targets, including p70S6 kinase, ribosomal S6, and 4E-binding protein-1. This

leads to increased translation of a specific subset of mRNAs, many of which are involved in cell cycle control (1, 10, 22). Loss of TSC2 affects the cell cycle, shortening G<sub>1</sub> and causing cells in G<sub>0</sub> to reenter the cell cycle (30). Biallelic mutations in either hamartin or tuberin result in diseases categorized by abnormal cellular proliferation, including TSC, an autosomal dominant tumor syndrome, and lymphangioleiomyomatosis (6, 29), a disease characterized by progressive accumulation of smooth muscle type cells in the lungs and lymphatics, generally leading to death by respiratory failure (16).

Although initially associated with a small number of rare diseases, tuberin is now recognized as an important modulator of cellular function, with roles in proliferation, hypertrophy, cytoskeletal organization, and nutrient sensing (27). Of particular relevance to airway smooth muscle cells is the recent findings that tuberin is phosphorylated by members of both the PI3K and mitogen-activated protein kinase (MAPK) pathways (28), and that the PI3K/Akt/mTOR pathway is required for airway smooth muscle differentiation and contractile protein expression (11). These findings suggest that tuberin may integrate mitogenic signaling in airway smooth muscle (3) and further that PI3K/Akt/mTOR and hence tuberin may be responsible for maintenance of smooth muscle phenotype. Despite this, little is known of the biology of tuberin in airway smooth muscle cells.

Tuberin is a 180-kDa protein with multiple phosphorylation sites for Akt (8, 14), adenosine monophosphate kinase (AMPK) (15), and MAPK2 (20). It also has a functional GAP domain for the small GTPase rheb (13, 34), multiple coiled coil domains, and a leucine zipper, consistent with protein interaction sites, but otherwise little homology with other proteins. Reports of tuberin's subcellular localization have been inconsistent: while most studies have described the protein as distributed diffusely throughout the cytoplasm (23, 26, 32), a small number have described tuberin in cytoplasmic vesicles or aggregates, attached to cytoskeletal components (33) and rarely the nucleus (21). These inconsistencies in the distribution of tuberin may be explained by the different cells and tissues studied, with the majority of reports examining transformed cell lines. We postulated that, to integrate these pathways in the airway smooth muscle cell, tuberin would have a complex pattern of subcellular localization, which was responsive to cellular status. To test this hypothesis, we examined the subcellular localization of tuberin in primary airway smooth muscle cells and how this changed through the cell cycle.

Address for reprint requests and other correspondence: S. R. Johnson, Division of Therapeutics and Molecular Medicine, Univ. of Nottingham, D floor, South block, Queens Medical Centre, Univ. Hospital, Nottingham NG7 2UH, UK (e-mail: simon.johnson@nottingham.ac.uk).

The costs of publication of this article were defrayed in part by the payment of page charges. The article must therefore be hereby marked "advertisement" in accordance with 18 U.S.C. Section 1734 solely to indicate this fact.

## MATERIALS AND METHODS

**Cell culture.** Human airway smooth muscle (HASM) cells were grown from explants of trachealis muscle from cadavers (donors died from nonrespiratory causes,  $n = 2$ ), as described (17), or from the large airways of surgical resection specimens ( $n = 1$ ). Ethical permission was received from the Queens Medical Centre Research Ethics Committee. Both airway smooth muscle and HeLa cells were grown in DMEM with 10% fetal bovine serum at 37°C and 5% CO<sub>2</sub>. For growth arrest of airway smooth muscle cells, this medium was replaced with DMEM without serum for 72 h. All experiments with airway smooth muscle cells were performed with cells between passages 6 and 10, at 50–70% confluence.

**Immunofluorescence and microscopy.** Cells were grown overnight on cover slips in six-well tissue culture plates, fixed for 10 min at room temperature with 4% paraformaldehyde in phosphate-buffered saline (PBS), and permeabilized with 0.2% Triton X-100 in PBS for 5 min at room temperature. Samples were blocked with 10% normal goat serum in PBS, then incubated with appropriate primary and secondary antibodies, with three 15-min washes in PBS after each incubation. After the final washes, the cover slips were rinsed briefly in distilled water and then mounted in Fluorescence Mounting Medium (DakoCytomation, Cambridgeshire, UK). Negative controls were preincubation of the antibody with the immunogenic peptide (tuberin N19), omission of the primary antibody, and an isotype control. The following antibodies were used at the dilutions indicated: antituberin N19 and C20 (1:100, Santa Cruz Biotechnology), antituberin d78, antituberin 5063 (1:100, Dr. J. DeClue, National Cancer Institute, Bethesda, MD), antinucleoli (1:40; MAB1277, Chemicon), FITC-conjugated goat anti-rabbit IgG (1:50; F1262, Sigma-Aldrich, Dorset, UK), and rhodamine-conjugated goat anti-mouse IgG (1:200, R6393, Cambridge BioScience, Cambridge, UK).

To label mitochondria, cells were incubated in 250-nm Mitotracker Deep Red 633 (Molecular Probes, Eugene, OR) in DMEM, with 10% fetal bovine serum at 37°C and 5% CO<sub>2</sub> for 45 min. The cells were then washed once with growth medium, fixed in 2% paraformaldehyde in growth medium for 15 min at 37°C, washed with PBS, and processed for immunofluorescence, as described above.

Standard epifluorescence microscopy was performed using a Zeiss Axiovert S100 microscope, and images were captured using a digital AxioCam and Axiovision software. Confocal microscopy was carried out using a Leica TCS4d confocal laser scanning microscope with an argon/krypton laser. The laser lines used were 488 nm (FITC), 568 nm (Rhodamine), and 633 nm (Mitotracker Deep Red).

**Flow cytometry.** Cells were removed from plates with trypsin, washed twice with PBS, fixed in 70% ethanol, and stored at –20°C. For analysis, cells were washed twice with PBS and then stained with 10 mg/ml propidium iodide (P4170, Sigma-Aldrich) in PBS. Cell cycle analysis was performed using a Becton Coulter Epics XL flow cytometer and WinMDI software.

**Cell fractionation.** One T75 flask of HASMs at 50% confluence was used per sample. Cells were scraped from flasks into PBS and washed twice in PBS and once in *buffer A* (10 mM Tris·Cl, pH 7.8, 10 mM KCl, 0.5 mM DTT, with protease and phosphatase inhibitors). Cell pellets were then gently resuspended in 100  $\mu$ l of *buffer A* plus 0.2% Igepal CA-630 (I3021, Sigma-Aldrich) and incubated on ice for 10 min. Nuclei were pelleted (10,000  $g$  for 10 min), and the supernatant was harvested as the cytoplasmic fraction. The nuclear pellet was washed twice in 200  $\mu$ l ice-cold *buffer A*, and the wash buffers were retained for analysis. Nuclei were then disrupted by trituration in 100  $\mu$ l of *buffer B* (20 mM Tris·Cl, pH 7.8, 150 mM NaCl, 50 mM KCl, 5 mM DTT, with protease and phosphatase inhibitors), and insoluble debris were removed by centrifugation (10,000  $g$  for 10 min). The supernatant was retained as the soluble nuclear fraction. The fractions were analyzed by Western blotting; wash buffers were also analyzed to monitor carry over of cytoplasm into the nuclear fraction. The data for the time course shown in Fig. 3

are representative of two experiments, performed on cells from a single donor.

**Western blotting.** Cell lysates were prepared by resuspending cell pellets in lysis buffer (50 mM Tris·Cl, pH 7.5, 150 mM NaCl, 1 mM EDTA, 1% Nonidet P-40), including protease and phosphatase inhibitors, for 15 min on ice and spinning out debris (10,000  $g$  for 10 min). Proteins were resolved by electrophoresis on 7.5% SDS-polyacrylamide gels and then blotted onto Hybond-P membrane (Amersham Biosciences, Buckinghamshire, UK) and probed with antituberin C20 and N19 (1:1,000) and antihamartin antibodies (1:1,000 Dr V. Ramesh, Massachusetts General Hospital, Boston, MA) using standard protocols. Other primary antibodies used include anti-B23/nucleophosmin (1:100; Sigma B0556), anti- $\alpha$ -tubulin (1:1,000; Sigma T5168), anti-p38 MAPK (1:1,000, New England Biolabs, no. 9212), anti-p42/44 MAPK (1:1,000, New England Biolabs, no. 9102), anti-Akt (1:1,000, New England Biolabs, no. 9272), anti-phospho-p38 MAPK (1:1,000, New England Biolabs, no. 9211S), anti-phospho-p42/44 MAPK (1:1,000, New England Biolabs, no. 9106), and anti-phospho-Akt (1:1,000, New England Biolabs, no. 4056P). Secondary antibodies were horseradish peroxidase-conjugated goat anti-rabbit IgG (1:20,000, Sigma-Aldrich) and horseradish peroxidase-conjugated goat anti-mouse IgG (1:1,000, Sigma-Aldrich). Signals were visualized using the ECL Western Blotting Detection Kit (Amersham Biosciences).

**Generation of tuberin-green fluorescent protein fusion constructs.** Four regions of the tuberin coding region were amplified by PCR using Platinum Pfx polymerase (Invitrogen, Paisley, UK). These regions corresponded to amino acids 1–450, 451–900, 901–1350, and 1351–1807. In each case, the upstream primer included a consensus Kozak sequence (19) and a methionine start codon, preceded by an *NheI* site for cloning into the vector. The downstream primer contained an *XhoI* site for cloning. The amplified fragments were digested with the restriction enzymes *NheI* and *XhoI* and cloned into the vector pEGFP-N1 (BD-Biosciences Clontech), which was also digested with *NheI* and *XhoI*. This resulted in the generation of a construct encoding green fluorescent protein (GFP) fused to the COOH-terminus of the chosen region of tuberin protein. Constructs were verified by sequencing.

**Transfection.** DNA for transfection was prepared using the Qiagen Spin Miniprep kit (Qiagen, West Sussex, UK). For transfection of HeLa cells, cells were plated into wells of six-well tissue culture plates at 60–80% confluence in DMEM with 10% FBS. Where cells were to be analyzed by microscopy, 22  $\times$  22 mm coverslips were placed in the wells before the cells were plated. Transfection was carried out using Fugene 6 transfection reagent (Roche Diagnostics, East Sussex, UK) or GeneJuice (Merck Biosciences, Nottingham, UK), according to the manufacturer's instructions. HASM cells were transfected using a Nucleofector (Amaxa, Cologne, Germany) and Basic Smooth Muscle Transfection Kit (Amaxa), according to the manufacturer's instructions. At 24 h posttransfection, cover slips were removed from the wells and the cells were fixed in 4% paraformaldehyde in PBS for 5 min at room temperature and then mounted in Fluorescence Mounting Medium (DakoCytomation).

**Fluorescence resonance energy transfer.** Fluorophore-tagged tuberin and hamartin constructs for fluorescence resonance energy transfer (FRET) were generated by PCR amplification of the entire coding regions of tuberin, hamartin, cyan fluorescent protein (CFP), and yellow fluorescent protein (YFP) using Accuprime DNA polymerase (Invitrogen, Paisley, UK). These fragments were cloned into pcDNA3.1 Zeo (Invitrogen). Tuberin was fused to CFP to generate tuberin-CFP, while hamartin was fused to YFP to generate YFP-hamartin and hamartin-YFP. Constructs were verified by sequencing and Western blotting to detect full-length product.

FRET was determined by acceptor photobleaching (18) in cells expressing both the donor- and the acceptor-tagged proteins. Samples were visualized using a Leica TCS SP2 Confocal Laser Scanning Microscope (Leica, Heidelberg, Germany), equipped with a DMIRBE

inverted microscope (Leica) with  $63 \times 1.32$  numerical aperture and  $40 \times 1.25$  numerical aperture oil immersion HCX Plan Apo objectives. CFP and YFP were excited using 458- and 514-nm laser lines, respectively. Detection parameters were optimized to eliminate cross talk. Prebleach images of CFP and YFP were captured, and then YFP was bleached in the region of interest (ROI) to  $\sim 50\%$  of its prebleach intensity by the 514-nm laser at 50% intensity using the Regulator function of the Leica Confocal Software Acceptor Photobleach module. Postbleach images were captured, and the increase in CFP signal (D) in the ROI was used to calculate the FRET efficiency ( $E_F$ ), according to the formula:  $E_F = (D_{\text{post}} - D_{\text{pre}})/D_{\text{post}}$ . Both YFP-hamartin and hamartin-YFP constructs were used in FRET experiments; FRET efficiencies from the hamartin-YFP construct were generally higher, and so data are presented for hamartin-YFP only. Control samples included CFP-tuberin only, which was subjected to a similar bleaching protocol to the experimental sample and showed no increase in CFP emission. Although values for FRET efficiencies are given in Fig. 5, measurements of donor fluorescence may be compromised by spectral bleed through of YFP emission into the CFP emission detection range, donor photobleaching, and autofluores-

cence, which is an issue in paraformaldehyde-treated samples. For this reason, the values given should be taken as a qualitative rather than quantitative indicator of FRET.

**Sequence analysis.** Protein database searching was carried out using BLAST [blastp] at <http://www.ncbi.nlm.nih.gov/BLAST/> (2). Potential nuclear and mitochondrial localization signals in tuberin were identified by the NUCDISC and MITDISC programs in PSORT II at <http://psort.nibb.ac.jp> (24).

## RESULTS

**Immunocytochemical staining of tuberin in primary airway smooth muscle cells.** A cycling population of airway smooth muscle cells was immunostained using antituberin N19. This showed tuberin was located in the cytoplasm and the nucleus of these cells. Within the nucleus of some cells, diffuse background staining with multiple intensely staining nuclear speckles was observed (Fig. 1, A and B). Cells rendered quiescent by serum deprivation, however, displayed little or no nuclear

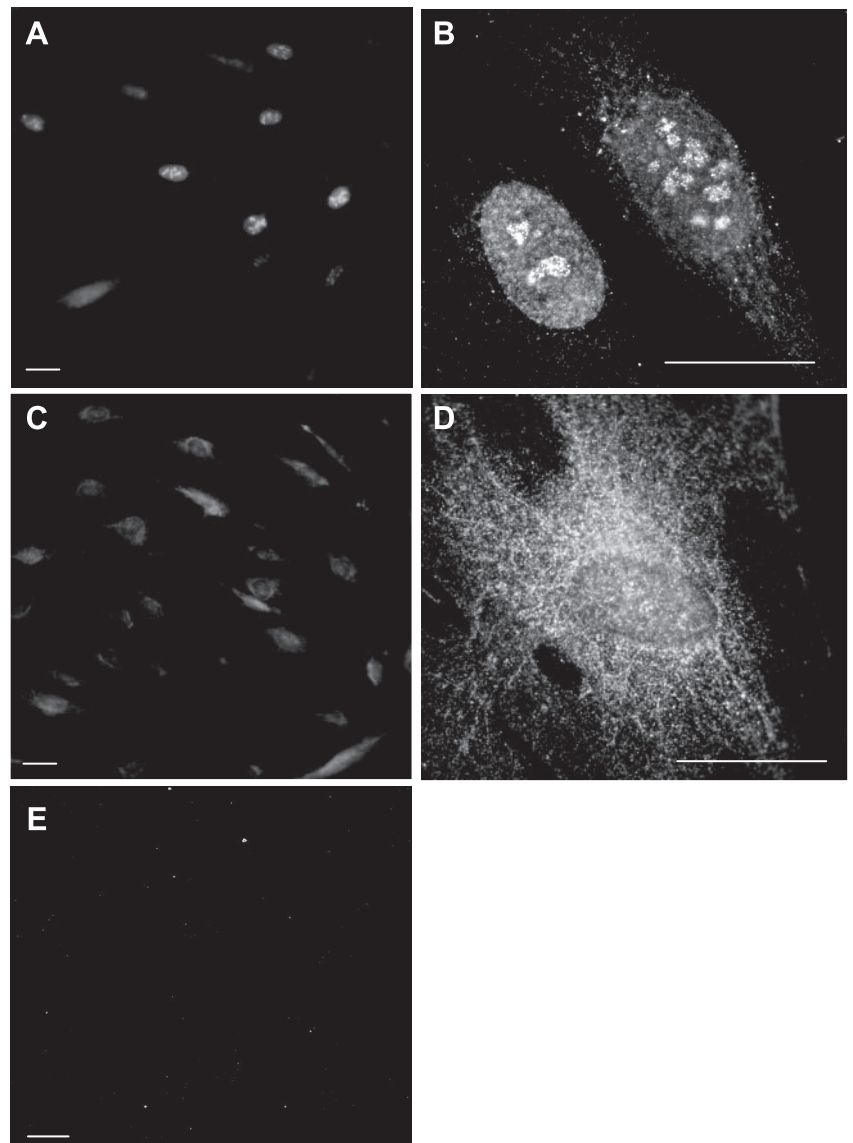


Fig. 1. Detection of tuberin in airway smooth muscle cells by immunofluorescence using antituberin N19 and a FITC-conjugated secondary antibody. A and B: cycling. C and D: quiescent airway smooth muscle cells. The distribution of tuberin as revealed by immunofluorescence differs between arrested and proliferating cells, with proliferating cells displaying more nuclear fluorescence. E: preincubation of the antibody with the immunogenic peptide inhibits tuberin immunofluorescence. Scale bar = 10  $\mu\text{m}$ .

immunofluorescence (Fig. 1, *C* and *D*). Control experiments, including omission of the primary antibody, use of an isotype control, and preincubation of the antibody with the immunogenic peptide, all inhibited this staining (Fig. 1*E*).

**Colocalization of tuberin with mitochondria.** In many cells, the cytoplasmic immunofluorescence was localized to discrete strandlike structures similar in morphology to mitochondria. Localization of tuberin to mitochondria has not been described in any cell type, and to confirm this localization we used three antisera directed at different epitopes on the tuberin molecule (antituberin C20, N19, and 5063), all of which detected these structures (only 5063 shown, Fig. 2). Dual immunofluorescence staining/confocal microscopy with Mitotracker Deep Red and antituberin 5063 demonstrated localization of tuberin on mitochondria (Fig. 2*A*).

**Colocalization of tuberin with nucleoli.** Since the speckled nuclear localization of tuberin had not previously been reported, we sought to identify the subnuclear compartment involved. At all stages in which tuberin speckles were present, they were found to colocalize with an antinucleolar antibody

(Fig. 2*B*). It was also noted that cells lacking tuberin speckles did not necessarily lack nucleoli, suggesting that tuberin was shuttling in and out of nucleoli, independent of the normal dissolution and reformation of the nucleolus during mitosis.

**Tuberin enters the nucleus during the  $G_1$  phase of the cell cycle.** The cycling population of airway smooth muscle cells had varying amounts of nuclear tuberin. As tuberin is a regulator of the cell cycle, which interacts with cyclin-dependent kinases and their inhibitors (7), we hypothesized that nuclear localization was dependent on the cell cycle. Nuclear and cytoplasmic fractions of synchronized airway smooth muscle cells were analyzed for tuberin by Western blotting using an antibody to the COOH-terminus of tuberin (antituberin C20). Cells growth arrested in  $G_0$  by serum deprivation were harvested for fractionation at 6-h intervals after stimulation by readdition of serum. Samples were taken simultaneously for analysis of DNA content by flow cytometry. Under these conditions, cells undergoing mitosis can be observed from 27-h poststimulation, with the 30-h time point containing pre- and postmitotic cells. For this reason, data are

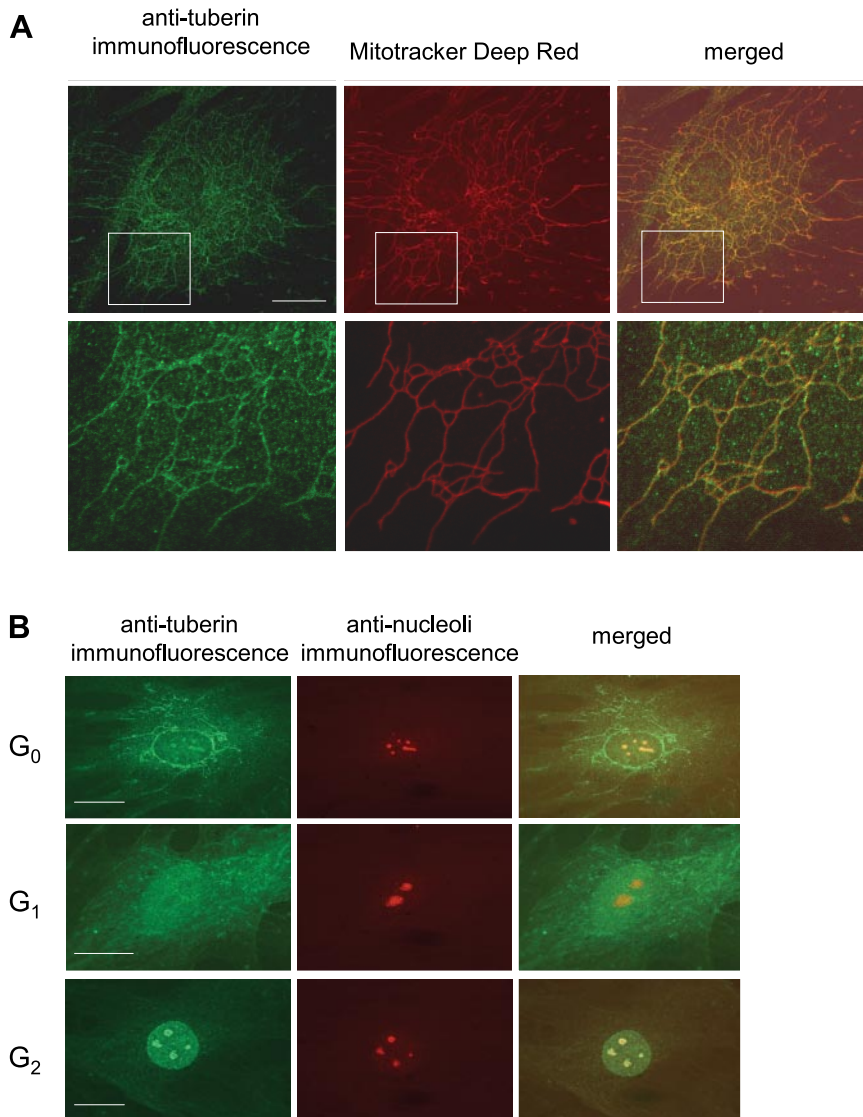
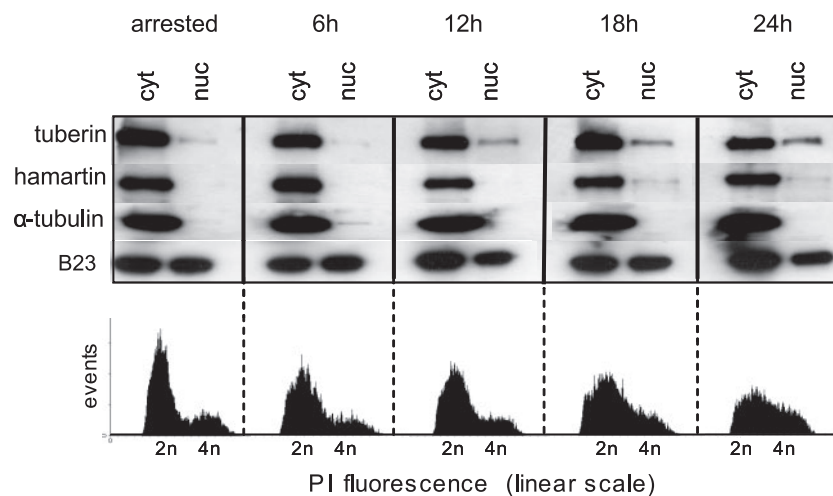


Fig. 2. *A*: tuberin colocalizes with mitochondria. Dual-fluorescent imaging of airway smooth muscle cells with antituberin 5063/FITC (green) and the mitochondrion-specific fluorescent dye Mitotracker Deep Red (red). White boxes show a magnified view of the indicated region of the larger image. The overlay (yellow) shows colocalization of tuberin immunofluorescence with mitochondria. Scale bar = 10  $\mu$ m. *B*: tuberin colocalizes with nucleoli. Images are of a representative single nucleus seen in a population of cycling airway smooth muscle cells. Tuberin was detected using antituberin N19 and a FITC-conjugated secondary antibody (green), while nucleoli were detected using an antinucleolar antibody with a rhodamine-conjugated secondary antibody (red). The overlay (yellow) shows colocalization of tuberin with nucleoli. Scale bar = 10  $\mu$ m.

Fig. 3. Nuclear localization of tuberin varies throughout the cell cycle. Airway smooth muscle cells were arrested by serum depletion for 72 h, restimulated by addition of 10% serum, and harvested at the indicated intervals. Nuclear (nuc) and cytoplasmic (cyt) protein fractions were immunoblotted for tuberin, hamartin,  $\alpha$ -tubulin, and B23. Cells were also examined for DNA content by propidium iodide (PI) staining and flow cytometry to demonstrate progression through the cell cycle (2n = diploid/G<sub>1</sub>, 4n = post S phase/G<sub>2</sub>). Tuberin enters the nucleus in G<sub>1</sub>, slightly before hamartin.



presented for 24 h of the cell cycle, only by which time the majority of the cells are in G<sub>2</sub> (Fig. 3).

Most tuberin is cytoplasmic, and total cellular tuberin does not vary significantly throughout the cell cycle. During G<sub>0</sub> and at 6 h poststimulation, tuberin is present at very low levels in the nuclear fraction, but accumulates in the nucleus from 12 h onwards (Fig. 3). Flow cytometry shows that the majority of these cells are still in G<sub>1</sub>. Since hamartin is known to interact with tuberin, hamartin was also examined and was found to enter the nucleus, although to a lesser extent than tuberin, and at a later point in the cell cycle [18 h poststimulation (Fig. 3)]. To detect contamination of the nuclear fraction by cytoplasm, blots were also probed with an antibody against the cytoplasmic protein  $\alpha$ -tubulin and with an antibody against B23/nucleophosmin to demonstrate equal loading of nuclear and cytoplasmic fractions, respectively. In addition, during the fractionation procedure, wash buffers were retained and monitored by Western blotting to ensure that washing of the nuclear pellet was adequate to remove residual cytoplasm (not shown).

*MAPK and Akt activation are not sufficient for nuclear localization of tuberin.* Others have shown that nuclear localization of tuberin is dependent on phosphorylation (21). As tuberin is phosphorylated at multiple sites by Akt and MAPK, we examined the role of these pathways in the nuclear localization of tuberin. Airway smooth muscle cells synchronized by serum depletion were stimulated with epidermal growth factor (EGF), platelet-derived growth factor (PDGF), insulin, or tumor necrosis factor- $\alpha$  (TNF- $\alpha$ ). Cells were processed for tuberin immunofluorescence 90 min and 24 h after the start of treatment. At 90 min, no rise in nuclear fluorescence was detected over control in any of the samples; after 24 h, increased nuclear fluorescence was detected in EGF- and PDGF-treated cells, but not TNF- $\alpha$  or insulin-treated cells (Fig. 4A). As MAPK-induced tuberin phosphorylation is likely to occur rapidly and nuclear translocation only occurred at the later time point with EGF and PDGF, which are smooth muscle mitogens, and not with TNF- $\alpha$ , which does not affect the cell cycle (4), we hypothesized that EGF and PDGF were promoting nuclear localization by causing cell cycle progression. To test this, airway smooth muscle cells synchronized by serum depletion were stimulated with EGF (20 ng/ml), with or without 2 mM hydroxyurea (which causes G<sub>1</sub> arrest), and harvested

for immunofluorescence after 24 h. Cells were stained with antituberin N19 and 4,6-diamidino-2-phenylindole, and a ratio of tuberin positive to total nuclei was scored in six low-power fields for each condition by a blinded observer. Preincubation of EGF-treated cells with hydroxyurea reduced the accumulation of nuclear tuberin by 47% ( $P = 0.004$ , Fig. 4B). In further experiments, cells were treated as above, and protein lysates were immunoblotted for total and phosphorylated p38, p42/44 MAPK, and Akt 18 h after stimulation. Unstimulated cells had very low or no detectable p38 MAPK, p42/44 MAPK, or Akt phosphorylation, and few cells had nuclear tuberin. Phospho-p38 was not detected 18 h after stimulation; however, EGF and PDGF treatment was associated with an increase in phosphorylated p42/44 MAPK, while EGF, and to a modest extent PDGF and insulin, were associated with increased phospho-Akt compared with serum-free medium. Hydroxyurea treatment did not significantly reduce the levels of phospho-p42/44 or phospho-Akt in response to these stimuli.

*Tuberin and hamartin colocalize in cytoplasmic speckles.* The speckled cytoplasmic distribution of tuberin we observed is similar to the distribution of hamartin in human embryonic kidney 293 cells, as described by Plank et al. (26). Furthermore, it was noted that cotransfection of tuberin-CFP and hamartin-YFP resulted in a redistribution of the normally diffusely cytoplasmic full-length tuberin-CFP into these speckles. This led us to hypothesize that tuberin was localized in these structures by hamartin binding. To test this hypothesis, we examined tuberin/hamartin binding in these speckles using FRET. HeLa cells were cotransfected with tuberin-CFP and hamartin-YFP expressing constructs and fixed 48 h posttransfection. Using acceptor photobleaching, we found that photobleaching YFP in ROI comprising cytoplasmic speckles consistently resulted in an increase in CFP emission with a FRET efficiency of 17% (SE 3.34,  $n = 15$ ). A CFP-only control had an apparent FRET efficiency of -3.8% (SE 5.0,  $n = 10$ ), which was significantly lower ( $P = 0.002$ ), indicating that hamartin and tuberin interact within these structures (Fig. 5).

*GFP-tuberin constructs colocalize to discreet subcellular fractions.* To confirm the subcellular localization of tuberin observed using immunofluorescence and fractionation/Western blotting and investigate how this differential localization is regulated, we transiently transfected HeLa cells with various tuberin-GFP constructs. Tuberin-GFP amino acids 1–450 only

(tuberin<sup>1-450</sup>-GFP) was cytoplasmic with focal speckles, tuberin<sup>451-900</sup>-GFP was diffusely cytoplasmic, tuberin<sup>901-1350</sup>-GFP selectively colocalized with mitochondria, and tuberin<sup>1351-1807</sup>-GFP was nuclear with perinucleolar enhance-

ment. Full length tuberin<sup>1-1807</sup>-GFP was diffusely cytoplasmic (Fig. 6A). To confirm that the subcellular distribution observed for these constructs was not an artifact of the use of HeLa cells, HASMs were transfected with the same constructs and pro-

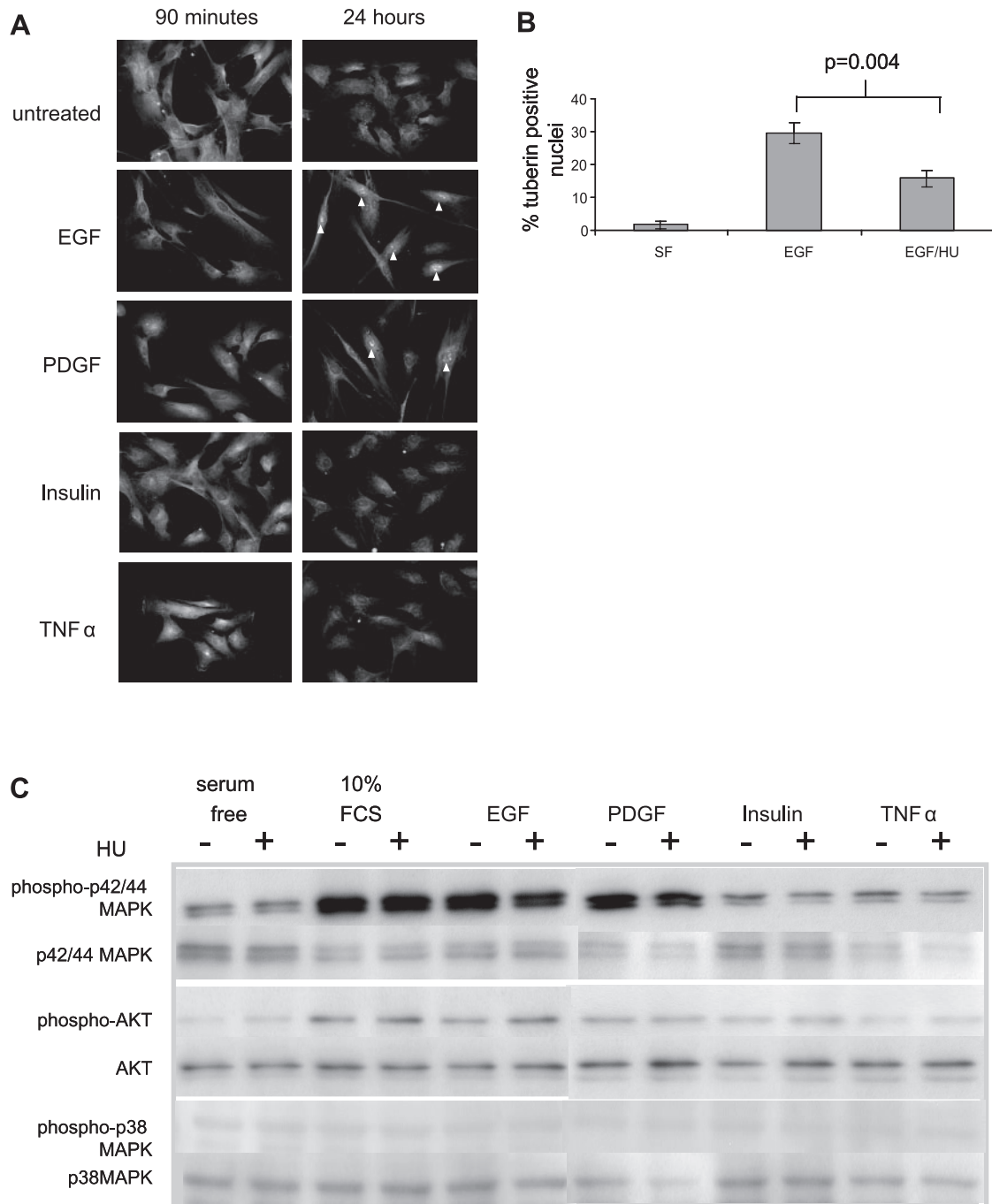


Fig. 4. A: stimulation of Akt and MAPK are not sufficient for nuclear import of tuberin. Airway smooth muscle cells were growth arrested and examined by immunofluorescence (tuberin N19) at 90 min and 24 h poststimulation with 20 ng/ml epidermal growth factor (EGF), 10 ng/ml platelet-derived growth factor (PDGF), 100 nM insulin, or 10 ng/ml TNF- $\alpha$ . Tuberin immunofluorescence was cytoplasmic at 90 min in all cases and became nuclear at 24 h in cells treated with PDGF and EGF but not in unstimulated, TNF- $\alpha$ , or insulin-treated cells. B: airway smooth muscle cells growth arrested by serum depletion were treated with serum-free (SF) medium, 20 ng/ml EGF, or EGF plus 2 mM hydroxyurea (HU), and harvested for antituberin immunofluorescence after 24 h. Results show means  $\pm$  SE of the ratio of tuberin positive to total nuclei. C: airway smooth muscle cells growth arrested by serum depletion were treated with SF medium (un), 10% fetal bovine serum, 20 ng/ml EGF, 10 ng/ml PDGF, 100 nM insulin, or 10 ng/ml TNF- $\alpha$ , with (+) and without (-) 2 mM HU, and harvested after 18 h for Western blotting with the antibodies indicated. At this time point, only basal levels of p38 MAPK phosphorylation were detected after each treatment, and this was not affected by HU. The phosphorylation of p42/44 MAPK in response to serum, EGF, and PDGF, and the phosphorylation of Akt in response to serum, EGF, PDGF, and insulin was maintained in the presence of HU.

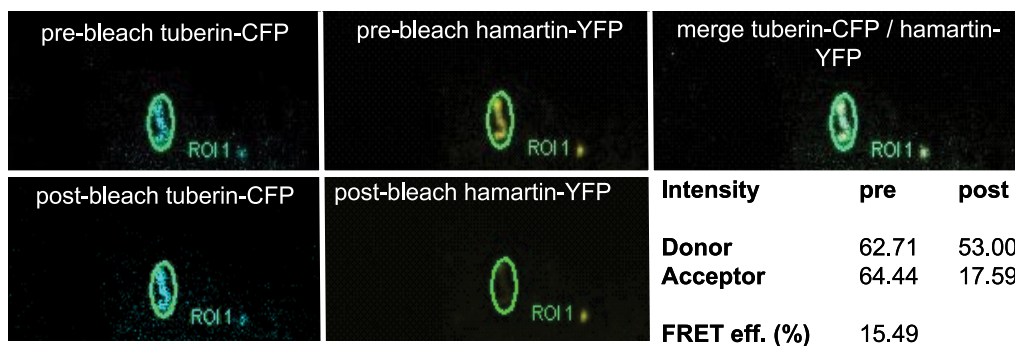


Fig. 5. Tuberin and hamartin colocalize and interact in cytoplasmic speckles. HeLa cells were cotransfected with tuberin-cyan fluorescent protein (CFP) and hamartin-yellow fluorescent protein (YFP)-expressing constructs. Figures show a tuberin/hamartin cytoplasmic speckle as the region of interest (ROI). YFP was photobleached in the ROI indicated by the oval, and pre- and postbleach measurements of CFP emission in the ROI compared with estimate fluorescence resonance energy transfer (FRET) efficiency. Figure shows prebleach images of tuberin-CFP (donor) and hamartin-YFP (acceptor). Merging images demonstrate colocalization of tuberin-CFP and hamartin-YFP. Postphotobleaching images of tuberin-CFP and hamartin-YFP show reduction of YFP relative intensity in the defined ROI. The table shows a single representative calculation of FRET efficiency in the defined ROI, where photobleaching of YFP in this region has resulted in an increase in CFP relative intensity of 15% (the mean FRET efficiency in this series of experiments was 17%).

duced similar results (Fig. 6B), with the exception that the expression of tuberin<sup>451-900</sup>-GFP was undetectable in these cells.

## DISCUSSION

We have shown that tuberin occupies multiple subcellular compartments, each mediated by specific regions of the protein. Two of these findings are novel in any cell type: first, that tuberin is selectively localized to mitochondria; and second, that cytoplasmic tuberin is translocated to the nucleus in G<sub>1</sub>. Furthermore, we show, using fluorophore-tagged tuberin and hamartin constructs and FRET analysis, that tuberin and hamartin interact in speckle-like cytoplasmic structures. Tuberin-GFP fusion proteins occupy specific cellular domains in HeLa cells and primary HASMs, demonstrating the presence of multiple localization sequences within the tuberin molecule. It is likely that these domains are of physiological importance, as immunofluorescent staining suggests that wild-type tuberin is located at these sites, at least transiently in airway smooth muscle cells.

The distribution of tuberin<sup>1301-1807</sup>-GFP suggests that the nuclear localization sequence is in the COOH-terminal 450 amino acids, as has previously been described (31). PSORT II identifies two potential nuclear localization sequences in this region, KKRH at amino acid position 1637, and PSRRGKR at 1468, which is adjacent to one of two Akt phosphorylation sites shown to be the major targets of the PI3K pathway in humans (22). However, our findings suggest that Akt phosphorylation alone cannot account in nuclear localization of tuberin, as insulin activated Akt more strongly than EGF, but only the latter resulted in nuclear localization. Hydroxyurea, an inhibitor of G<sub>1</sub>-G<sub>2</sub> progression, reduced nuclear localization of tuberin in response to EGF without significantly affecting Akt and p42/44 MAPK phosphorylation. In addition, PDGF and insulin treatment resulted in a similar modest increase in Akt phosphorylation, but only PDGF treatment resulted in nuclear accumulation of tuberin. Taken together, our findings suggest that progression through the cell cycle is required for nuclear localization, and, although we cannot exclude a role for Akt, p38, and p42/44 MAPKs, their activation is not sufficient for nuclear localization of tuberin, which may occur in response to

phosphorylation by cell cycle regulatory proteins. How might these observations correlate with the observed effects of tuberin loss on the cell cycle? The relocation of tuberin into nuclei occurs during late G<sub>1</sub>; Soucek et al. (30) found that absence of tuberin can both induce G<sub>1</sub>/S transition and prevent cells from entering G<sub>0</sub>; thus inhibition of G<sub>1</sub>/S transition may correspond with nuclear import of tuberin during G<sub>1</sub>.

We were unable to recapitulate the nucleolar localization of tuberin seen with the antituberin N19 antiserum using GFP fusion proteins. In addition, other antituberin antisera do not detect nucleoli to any significant degree, raising the possibility that this aspect of the distribution of tuberin in airway smooth muscle cells is an artifact of this particular antiserum. However, tuberin<sup>1301-1807</sup>-GFP shows a distinct perinucleolar distribution (arrowed in Fig. 6A), and so it is also possible that, in creating the deletion derivatives of tuberin, we have separated nuclear and nucleolar targeting sequences, such that the nucleolar targeting sequence is located in one of the tuberin-GFP constructs, which is unable to enter the nucleus.

Endogenous tuberin was identified on mitochondria by a panel of antibodies raised against different epitopes of the protein. Moreover, tuberin<sup>901-1350</sup>-GFP was specifically found on mitochondria, suggesting a mitochondrial targeting signal (MTS) to be within this part of the molecule. The NH<sub>2</sub>-terminus of this construct fortuitously contains a canonical MTS (detected by PSORT II). Such positively charged presequences are generally present at the NH<sub>2</sub>-terminus of mitochondrial proteins and are cleaved on entry into the mitochondrion [reviewed by Brunner et al. (5)]. The NH<sub>2</sub>-terminal MTS on the tuberin<sup>901-1350</sup>-GFP protein is not a terminal sequence in wild-type tuberin, raising the possibility that it does not function as an MTS in the full-length protein. However, presequence-like MTS can also be located away from the NH<sub>2</sub>-terminus of the protein (9). Intriguingly, this fragment contains the two AMPK phosphorylation sites, S1345 and T1227 (Fig. 6C), and may implicate mitochondrial localization of tuberin with energy sensing via AMPK.

The tuberin<sup>1-450</sup>-GFP protein was cytoplasmic with focal speckles and mimics the punctate cellular distribution described for hamartin (26). Tuberin<sup>1-450</sup>-GFP contains the coiled coil hamartin binding domain (25), and using FRET we

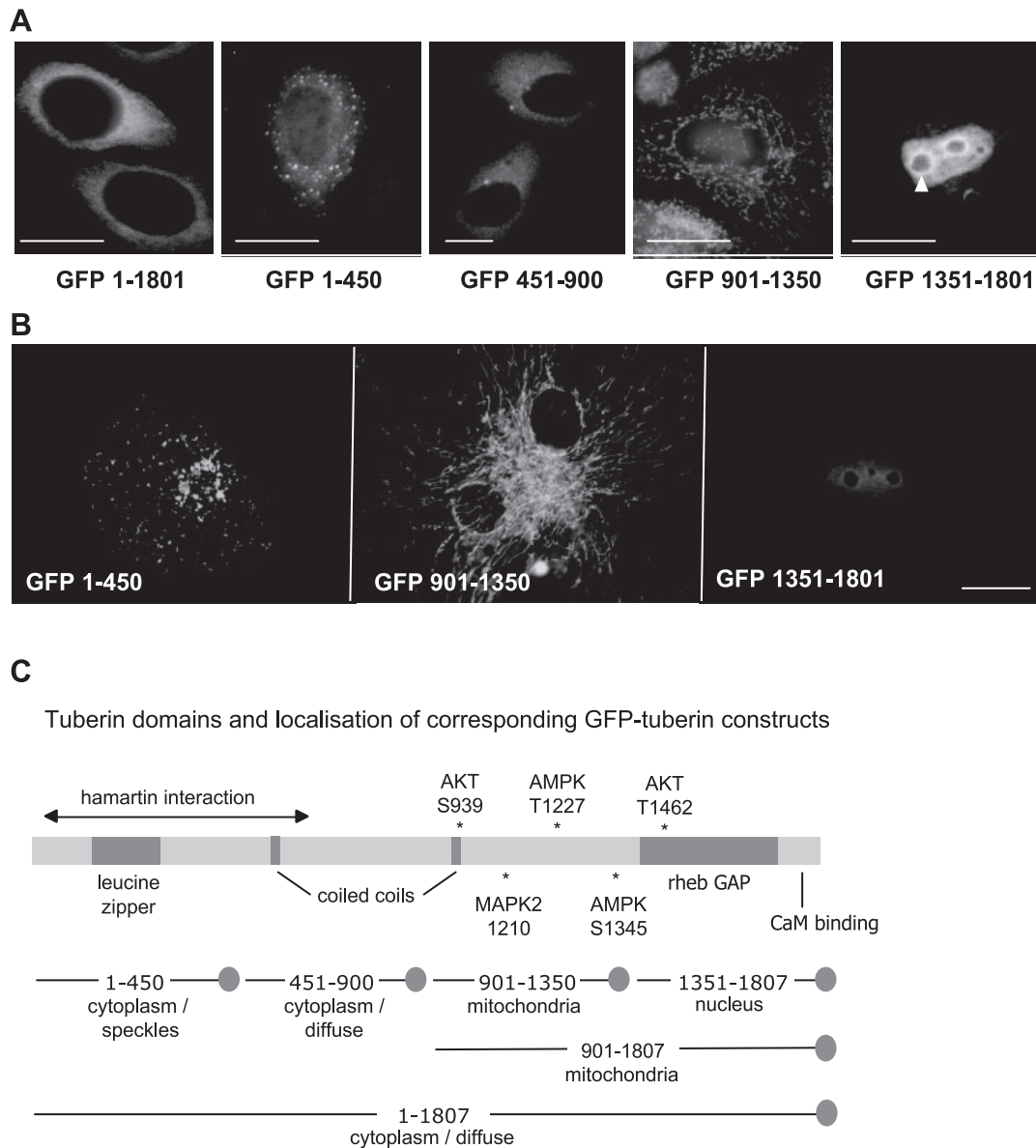


Fig. 6. Transfection of tuberin-green fluorescent protein (GFP) expressing constructs reveals multiple subcellular localization sequences in the tuberin protein. Scale bar = 10  $\mu$ m. **A:** HeLa cells transfected with tuberin-GFP constructs comprising full length and four sections of the tuberin protein (amino acids 1–450, 451–900, 901–1300, 1301–1807, and 1–1807). Arrow indicates perinucleolar accumulation of tuberin<sup>1301–1807</sup>-GFP. **B:** human airway smooth muscle (HASM) cells transfected with tuberin-GFP constructs encoding amino acids 1–450, 901–1300, and 1301–1807. **C:** schematic representation of the tuberin-GFP constructs: subcellular localization and known corresponding protein domains. CaM, calmodulin; GAP, GTPase activating protein; AMPK, adenosine monophosphate kinase. \*Phosphorylation sites at specific amino acid residues. S, serine; T, threonine.

showed a direct tuberin/hamartin interaction between the two full-length proteins in these speckles, providing a mechanism for this localization. Other subcellular tuberin locations, including mitochondria and nucleus, are independent of the hamartin binding domain and may occur preferentially when tuberin/hamartin have dissociated (1), thus allowing other interactions. The use of FRET has allowed us to confirm the tuberin/hamartin interaction at a subcellular level within specific cellular domains.

Tuberin is a large protein with multiple protein interactions and postulated roles (27). The complexity of these proposed tuberin interactions is likely to be at least partly regulated by selective subcellular localization of tuberin and its interacting

proteins. Our study is supportive of this idea, as the protein has domains targeting multiple subcellular sites, which can be regulated dynamically (e.g., by the cell cycle), allowing transient interactions with different groups of proteins. Proteins with multiple transient protein/protein interactions are termed “date hubs” and tend to be important regulatory proteins (12). This observation, together with evidence that tuberin is a target of major airway smooth muscle signaling pathways, suggests tuberin has a role in integrating mitogenic signals, smooth muscle proliferation, cell size, and migration, thus being relevant to diseases such as asthma, in addition to those where tuberin function is absent, such as lymphangioma- leiomyomatosis.

## ACKNOWLEDGMENTS

We thank Jeff deClue, Dan Noonan, Brendan Manning, and Vijaya Ramesh for reagents; Richard Lamb for protocols and helpful comments; Tim Self and Kelly Draper-Morgan for assistance with confocal microscopy; and Joel Moss and Alan Knox for help and advice.

## GRANTS

D. Clements is funded by lymphangioleiomyomatosis (LAM) Action. The study was funded by the LAM Action, University Hospital Special Trustees, and the University of Nottingham.

## REFERENCES

- Aicher LD, Campbell JS, Yeung RS. Tuberin phosphorylation regulates its interaction with hamartin. Two proteins involved in tuberous sclerosis. *J Biol Chem* 276: 21017–21021, 2001.
- Altschul S, Gish W, Miller W, Myers E, Lipman D. Basic local alignment search tool. *J Mol Biol* 215: 403–410, 1990.
- Ammit AJ, Panettieri RA Jr. Signal Transduction in Smooth Muscle: Invited Review: The circle of life: cell cycle regulation in airway smooth muscle. *J Appl Physiol* 91: 1431–1437, 2001.
- Amrani Y, Panettieri R Jr, Frossard N, Bronner C. Activation of the TNF alpha-p55 receptor induces myocyte proliferation and modulates agonist-evoked calcium transients in cultured human tracheal smooth muscle cells. *Am J Respir Cell Mol Biol* 15: 55–63, 1996.
- Brunner M, Schneider HC, Lill R, Neupert WP. Dissection of protein translocation across the mitochondrial outer and inner membranes. *Cold Spring Harb Symp Quant Biol* 60: 619–627, 1995.
- Carsillo T, Astrinidis A, Henske EP. Mutations in the tuberous sclerosis complex gene TSC2 are a cause of sporadic pulmonary lymphangioleiomyomatosis. *Proc Natl Acad Sci USA* 97: 6085–6090, 2000.
- Catania MG, Mischel PS, Vinters HV. Hamartin and tuberin interaction with the G2/M cyclin-dependent kinase CDK1 and its regulatory cyclins A and B. *J Neuropathol Exp Neurol* 60: 711–723, 2001.
- Dan HC, Sun M, Yang L, Feldman RI, Sui XM, Ou CC, Nellist M, Yeung RS, Halley DJJ, Nicosia SV, Pledger WJ, Cheng JQ. Phosphatidylinositol 3-kinase/Akt pathway regulates tuberous sclerosis tumor suppressor complex by phosphorylation of tuberin. *J Biol Chem* 277: 35364–35370, 2002.
- Folsch H, Guiard B, Neupert W, Stuart RA. Internal targeting signal of the BCS1 protein: a novel mechanism of import into mitochondria. *EMBO J* 15: 479–487, 1996.
- Goncharova EA, Goncharov DA, Eszterhas A, Hunter DS, Glassberg MK, Yeung RS, Walker CL, Noonan D, Kwiatkowski DJ, Chou MM, Panettieri RA Jr, Krymskaya VP. Tuberin regulates p70 S6 kinase activation and ribosomal protein S6 phosphorylation. A role for the TSC2 tumor suppressor gene in pulmonary lymphangioleiomyomatosis (LAM). *J Biol Chem* 277: 30958–30967, 2002.
- Halayko AJ, Kartha S, Stelmack GL, McConville J, Tam J, Camoretti-Mercado B, Forsythe SM, Hershenson MB, Solway J. Phosphatidylinositol-3 kinase/mammalian target of rapamycin/p70S6K regulates contractile protein accumulation in airway myocyte differentiation. *Am J Respir Cell Mol Biol* 31: 266–275, 2004.
- Han JD, Bertin N, Hao T, Goldberg DS, Berriz GF, Zhang LV, Dupuy D, Walhout AJ, Cusick ME, Roth FP, Vidal M. Evidence for dynamically organized modularity in the yeast protein-protein interaction network. *Nature* 430: 88–93, 2004.
- Inoki K, Li Y, Xu T, Guan KL. Rheb GTPase is a direct target of TSC2 GAP activity and regulates mTOR signaling. *Genes Dev* 17: 1829–1834, 2003.
- Inoki K, Li Y, Zhu T, Wu J, Guan K. TSC2 is phosphorylated and inhibited by Akt and suppresses mTOR signalling. *Nat Cell Biol* 4: 648–657, 2002.
- Inoki K, Zhu T, Guan KL. TSC2 mediates cellular energy response to control cell growth and survival. *Cell* 115: 577–590, 2003.
- Johnson S. Rare diseases. 1. Lymphangioleiomyomatosis: clinical features, management and basic mechanisms. *Thorax* 54: 254–264, 1999.
- Johnson S, Knox A. Autocrine production of matrix metalloproteinase-2 is required for human airway smooth muscle proliferation. *Am J Physiol Lung Cell Mol Physiol* 277: L1109–L1117, 1999.
- Karpova TS, Baumann CT, He L, Wu X, Grammer A, Lipsky P, Hager GL, McNally JG. Fluorescence resonance energy transfer from cyan to yellow fluorescent protein detected by acceptor photobleaching using confocal microscopy and a single laser (Abstract). *J Microsc* 209: 56, 2003.
- Kozak M. At least six nucleotides preceding the AUG initiator codon enhance translation in mammalian cells. *J Mol Biol* 196: 947–950, 1987.
- Li Y, Inoki K, Vaccrasis P, Guan KL. The p38 and MK2 kinase cascade phosphorylates tuberin, the tuberous sclerosis 2 (TSC2) gene product, and enhances its interaction with 14–3-3. *J Biol Chem* 278: 13663–13671, 2003.
- Lou D, Griffith N, Noonan DJ. The tuberous sclerosis 2 gene product can localize to nuclei in a phosphorylation-dependent manner. *Mol Cell Biol Res Commun* 4: 374–380, 2001.
- Manning BD, Tee AR, Logsdon MN, Blenis J, Cantley LC. Identification of the tuberous sclerosis complex-2 tumor suppressor gene product tuberin as a target of the phosphoinositide 3-kinase/akt pathway. *Mol Cell* 10: 151–162, 2002.
- Murthy V, Haddad LA, Smith N, Pinney D, Tyszkowski R, Brown D, Ramesh V. Similarities and differences in the subcellular localization of hamartin and tuberin in the kidney. *Am J Physiol Renal Physiol* 278: F737–F746, 2000.
- Nakai K, Kanehisa M. A knowledge base for predicting protein localization sites in eukaryotic cells. *Genomics* 14: 897–911, 1992.
- Nellist M, van Slegtenhorst MA, Goedbloed M, van den Ouweland AM, Halley DJJ, van der Sluijs P. Characterization of the cytosolic tuberin-hamartin complex. Tuberin is a cytosolic chaperone for hamartin. *J Biol Chem* 274: 35647–35652, 1999.
- Plank TL, Yeung RS, Henske EP. Hamartin, the product of the tuberous sclerosis 1 (TSC1) gene, interacts with tuberin and appears to be localized to cytoplasmic vesicles. *Cancer Res* 58: 4766–4770, 1998.
- Rosner M, Freilinger A, Hengstschlager M. Proteins interacting with the tuberous sclerosis gene products. *Amino Acids (Vienna)* 27: 119–128, 2004.
- Roux PP, Ballif BA, Anjum R, Gygi SP, Blenis J. Tumor-promoting phorbol esters and activated Ras inactivate the tuberous sclerosis tumor suppressor complex via p90 ribosomal S6 kinase. *Proc Natl Acad Sci USA* 101: 13489–13494, 2004.
- Sepp T, Yates JR, Green AJ. Loss of heterozygosity in tuberous sclerosis hamartomas. *J Med Genet* 33: 962–964, 1996.
- Soucek T, Pusch O, Wienecke R, DeClue JE, Hengstschlager M. Role of the tuberous sclerosis gene-2 product in cell cycle control. Loss of the tuberous sclerosis gene-2 induces quiescent cells to enter S phase. *J Biol Chem* 272: 29301–29308, 1997.
- Tsuchiya H, Orimoto K, Kobayashi K, Hino O. Presence of potent transcriptional activation domains in the predisposing tuberous sclerosis (Tsc2) gene product of the Eker rat model. *Cancer Res* 56: 429–433, 1996.
- Wienecke R, Maize JC Jr, Reed JA, de Gunzburg J, Yeung RS, DeClue JE. Expression of the TSC2 product tuberin and its target Rap1 in normal human tissues. *Am J Pathol* 150: 43–50, 1997.
- Yamamoto Y, Jones KA, Mak BC, Muehlenbachs A, Yeung RS. Multicompartmental distribution of the tuberous sclerosis gene products, hamartin and tuberin. *Arch Biochem Biophys* 404: 210–217, 2002.
- Zhang Y, Gao X, Saucedo LJ, Ru B, Edgar BA, Pan D. Rheb is a direct target of the tuberous sclerosis tumour suppressor proteins. *Nat Cell Biol* 5: 578–581, 2003.